

GENETIC ALGORITHM–BASED CO-OPTIMIZATION OF PV AND ESS FOR IMPROVED VOLTAGE STABILITY AND POWER SYSTEM RESILIENCE

Nur Bağnu Polat^{1*}, İlker Dursun², Sezgin Kaçar³

¹ Sakarya University of Applied Sciences, Faculty of Technology, Department of Electrical and Electronics Engineering, Esentepe Kampüsü, Serdivan, 54050, Türkiye

² Sakarya University of Applied Sciences, Faculty of Technology, Department of Electrical and Electronics Engineering, Esentepe Kampüsü, Serdivan, 54050, Türkiye

³ Sakarya University of Applied Sciences, Faculty of Technology, Department of Electrical and Electronics Engineering, Esentepe Kampüsü, Serdivan, 54050, Türkiye

Abstract

The penetration of renewable energy sources not only increases the flexibility of power systems but also brings stability issues. In particular, the irregular nature of photovoltaic (PV) production reduces system reliability by causing voltage fluctuations and power losses in the grid. Energy storage systems (ESS) support system stability by compensating for these fluctuations. However, optimising the placement capacity is critical, as the random placement of PV and ESS reduces system performance.

This study proposes a PV-ESS optimisation method to improve the stability of power systems, supported by sensitivity analysis. The proposed approach has been implemented on IEEE 9, 14, and 30 busbar test systems. The approach determines the weakest busbars in the system and selects the most appropriate locations and sizes for PV-ESS. Using a multi-objective optimisation method, the active power loss, voltage deviation, and stability index of the devices placed at the selected locations are at the same time minimised. System reactions were tested using N-1 emergency analyses. The results show that for Case 9, total losses decreased by 8% while system stability increased by 57%. For Case 14, P_{loss} decreased by 60% while stabilization increased by 74%. For Case 30, P_{loss} decreased by 11% while stabilization increased by 5%. These results show that the suggested method not only improves stability but also enhances the impact of PV-ESS integration on power system resilience.

The following chapters of the article are organised as follows: Section 2 surveys current literature on voltage stability in power systems and PV-ESS integration. Section 3 explains the proposed Genetic Algorithm (GA)-based PV-ESS co-optimisation methodology in detail and describes the L-index-based location determination and multi-objective sizing process. Section 4 presents simulation results obtained on IEEE 9, 14, and 30-bus test systems and discusses the achieved performance improvements. Section 5 includes a discussion, results, and recommendations for future work.

Keywords: Voltage Stability, N-1, L-index, Genetic Algorithm, PV-ESS Co-optimization

1. INTRODUCTION

The continuous, safe and economical delivery of electrical energy to end customers is the main goal of modern power systems. Increasing energy consumption and the accelerated penetration of renewable sources have complicated the dynamic nature of networks, making energy stability and quality issues more visible. In particular, the increasing share of inverter-based generation units in the system leads to voltage fluctuations, insufficient reactive power support, and

stability issues (Ülger & Dağ, 2024). Therefore, voltage stability has become a critical performance criterion in today's power systems (Kundur, 1994; Tachibana et al., 2014; Wu, 2007; Ajjarapu & Lee, 1998). The voltage instability is mainly a result of factors such as structural vulnerabilities of the power system, lack of reactive power support, failure to provide adequate compensation, or unexpected operational behaviour of tap-changing transformers. This situation can lead to serious outcomes, ranging from partial blackouts to widespread system collapse, by leading to gradual

*Corresponding author: Nur Bağnu Polat, nurbagnupolat@subu.edu.tr



© 2025 by the authors. This article is an open access article distributed under the terms and conditions of the Creative Commons Attribution (CC BY) license (<https://creativecommons.org/licenses/by/4.0/>).

or abrupt voltage drops in the system. For this reason, it is essential to identify the most vulnerable points in the grid, which are the most sensitive positions, and to analyze the voltage response of these busbars in order to assess stability correctly.

In recent years, the concept of power system resilience has gained increasing importance as a complementary element of stability studies. Power system resilience is defined as the system's capacity to maintain its essential functions or mitigate the intensity and impact of an unexpected event (Stanković et al., 2022). With the widespread adoption of renewable energy sources, ESSs have been shown to become not only a stability-enhancing element but also a component capable of supporting black-start-like processes in emergencies (Abdolahi et al., 2025; Zhao et al., 2022). Therefore, it is now accepted that ESSs contribute to all phases of event preparation, operational support during an event, and post-event reconstruction (Aslam et al., 2025).

This study proposes a genetic algorithm (GA)-based integrated optimisation algorithm that addresses the integration of PV and ESS into the power system from both stability and resilience aspects, to address this gap in the literature. The proposed approach;

- Determines the vulnerability analysis of the grid by identifying the weakest points in the system using the L-index method;
- Optimises the optimal locations and power capacities of PV and ESS simultaneously
- Improves voltage stability, power loss and voltage profile indicators together using a multi-objective function,
- Finally, it quantitatively demonstrates the methodology's impact on system resilience through N-1 emergency analyses

This study thus offers a novel approach to PV-ESS optimization, not only in terms of energy efficiency but also by addressing stability and resilience as an integrated approach, thus contributing to the current literature.

2. LITERATURE REVIEW

Voltage stability analyses are generally classified as static and dynamic approaches. In static analyses, the maximum capacity of the system for power transfer is determined through power flow solutions. Dynamic analyses examine the temporal effects of transient events on voltage stability (Gao et al., 1993; Ekinici, 2015). Among these approaches, static methods appear to be the most widely used tools for assessing voltage limits. A number of techniques for static voltage stability analysis have been proposed in the literature. The most popular techniques are the PV (P-V) curve method, the QV (Q-V) curve method, the Jacobian matrix determinant method, and the L-index method (Hsiao et al., 1994; Chen & Liu, 1994; Xiong et al., 2008). PV-QV curve methods are the most

widely used methods for determining the load limits and critical points of all busbars in the system under steady-state conditions (Ramasamy et al., 2016; Al Jabri et al., 2015; Zare & Kazem, 2007). PV curves analyze the relationship between active power and voltage to analyze the system's instability point and the maximum active power that can be transmitted. QV curves analyze the relationship between reactive power and voltage and analyze the reactive power margin and, therefore, the compensation requirements (Overby & Dobson, 1994). The L-index is a method used to evaluate the distance of a system from its stability limit based on power flow analysis (Chen et al., 2014). With values ranging from 0 to 1, the L-index indicates the distance of the system from its stability limit; values closer to 1 indicate that the system is approaching the voltage collapse limit. Research shows that more appropriate voltage stability analyses can be achieved by simultaneously evaluating active and reactive power (Taylor, 1994).

The impact of photovoltaic (PV) generation and energy storage systems (ESS) on improving voltage stability has become a significant area of research. Studies in this field show that properly positioned and correctly sized ESSs significantly contribute to the system by providing active and reactive power support to the load buses. Leonardi and Ajarapu increased the system's resilience to voltage sags by optimizing battery power sources using a control approach based on reactive power reserve sensitivities (Leonardi and Ajarapu, 2013). These studies emphasize that voltage stability analysis in power systems should be considered not only in relation to static limits but also to operational flexibility and resilience.

3. MATERIALS AND METHODS

In this paper, an integrated optimization algorithm has been developed for the optimal location and dimensioning of photovoltaic (PV) and energy storage systems (ESS) on IEEE standard test systems. The Algorithm aims to increase the system's voltage stability and reduce power losses. The MATPOWER 8.0 library has been used for the analysis. All the experiments have been carried out on the IEEE 9-bus (case 9), IEEE 14-bus (case 14), and IEEE 30-bus (case 30) test systems, which are commonly used in the literature.

The model proposed in this article has an integrated approach that addresses the integration of PV and ESS into the power system in terms of stability and resilience. It addresses the integration of PV and ESS into the power system in terms of stability and resilience. The model consists of two main steps:

- **L-index-based positioning stage:** In this step, the worst busbars in the system are identified, and the optimal locations for PV and ESS are identified.
- **Genetic Algorithm (GA)-based sizing step:** PV and ESS capacity are not only optimized at the specified locations, but the system's voltage

stability (maximum L-index), efficiency (active power loss), and voltage profile (average deviation) are also optimized.

The interoperability of these two case allows PV-ESS integration to improve not only energy quality but also the system's N-1 security and flexibility capabilities. The proposed approach contributes to more flexible and resilient power system operation by combining stability, efficiency, and reliability within a single optimization framework.

3.1 Baseline scenario and vulnerability analysis

To quantitatively assess the effectiveness of the optimization methodology proposed, the first step was to analyze the existing state of each IEEE test system (9, 14, and 30 bar) under study, i.e., as it is currently without photovoltaic (PV) or energy storage system (ESS) integration. This "Baseline" analysis serves as a basic benchmark for determining the natural system's operational weaknesses and then to measure the success of the applied improvements. At this step, system performance was analysed using three key indicators: maximum voltage stability index (L_{max}), total active power loss ($P_{loss,base}$) and average voltage deviation (ΔV_{avg}). These three parameters formed the main performance criteria for the optimization in subsequent sections. The L index is computed as in Equation 1 for any load drop.

$$L_j = 1 - \sum_{i=1}^{NPV} F_{ji} \frac{V_i}{V_j}$$

Here, L_j refers to the load node, NPV refers to the number of generator buses, NPQ refers to the number of load buses. The following intermediate statements are used in calculating the L index:

$$F_{LG} = Y_{LL}^{-1} Y_{LG}$$

$$V_L = Z_{LL} I_L + F_{LG} V_G$$

$$\begin{bmatrix} I_G \\ I_L \end{bmatrix} = \begin{bmatrix} Y_{GG} & Y_{GL} \\ Y_{LG} & Y_{LL} \end{bmatrix} \begin{bmatrix} V_G \\ V_L \end{bmatrix}$$

$$I = YV$$

Y: Node admittance matrix (Y-bus matrix)

I and V: Current and voltage vectors.

3.2 Optimal Position Determination (PV – ESS)

The PV and ESS locations were determined using a L-index minimisation-based systematic search method. Active power was injected into each PQ busbar at a certain rate in order, and the variation in L_{max} was monitored. The busbar with the lowest value was chosen as the best location. In this context, the PV and ESS locations were determined as follows

3.2.1 Determining The Pv Location

A test PV generator was added to all load bars (PQ bars) in order, at a percentage of the total system load (e.g. 18%). The PV power was set at 18% of the system power, and this choice stemmed from preliminary sensitivity analyses and was used only as an initial test value to observe system behavior. For each test, the power flow was run to compute the system's maximum L-index L_{max} . The busbar providing the lowest L_{max} value was identified as the most appropriate location for the PV system. Additional tests performed with different α penetration values confirmed that the selected PV location remained unchanged.

3.2.2 Determining The Pv Location

After the PV system was fixed in its optimal position, a same procedure was applied for the ESS. A test ESS (modelled as a generator) was applied to the PV system in turn to all load bars, and the bar with the lowest value of L_{max} was selected as the optimal position for the ESS. The test powers were 8% (like PV system). ESS; $V=1.03$ p.u. was fixed for PV and $V=1.02$ p.u. for ESS. These values were selected following preliminary sensitivity tests performed over the 1.00–1.05 p.u. range, which showed that variations within this interval had a negligible effect on both L_{max} and the overall bus voltage profile.

3.3 Genetic Algorithm–Based Sizing

In this stage of the study, after identifying the optimal locations for PV and ESS, a Genetic Algorithm (GA) was adopted to optimize the active power amounts these units would contribute to the system. In the literature, similarly, capacity ratios normalised according to the system load have been identified in PV-ESS size optimizations (Cho et al., 2024; Liu et al., 2023). This approach is essential in terms of both comparability and measurability. In similar studies in the literature, energy quality metrics such as active power loss, voltage deviation, or PV penetration have generally been used as priority optimisation targets (Qi et al., 2024; Wang et al., 2025).

$$\alpha = \frac{P_{pv}}{P_{toplam}}, \beta = \frac{P_{EDS}}{P_{toplam}} \quad (6)$$

3.3.1 Definition of Optimization Variables (α and β)

The purpose of the GA is to simultaneously improve the overall performance of the system by optimizing the PV and ESS power ratios (α and β). In this paper, the optimization variables are defined as a percentage of the total load, as shown in Equation 6. In this paper, the focus is on the voltage stability of the system, and the L-index is emphasised as the main performance metric. The α and β coefficients used refer to the rate at which PV and ESS capacities cover

the total load in the system.

3.3.2 Multi-Objective Fitness Function and Penalty Mechanism

The optimization objective function consists of three parameters: maximum L-index (L_{max}), normalized active power loss ($P_{loss}/P_{loss,base}$) and mean voltage deviation (ΔV_{ava}) The three performance measures are assigned weights as shown in Equation 7:

$$F_{min} = w_1 \cdot L_{max} + w_2 \cdot \frac{P_{loss}}{P_{loss,base}} + w_3 \cdot \Delta V_{ort}$$

In the aim function shown in Equation 7, (L_{max}), is the maximum voltage stability index of the system. (P_{loss}) is the active power loss in the last state, while (ΔV_{ava}) refers to the total absolute variation of the voltages across all buses from their nominal values.

The penalty coefficient is the value added when bus voltages are outside the operational boundaries. To ensure that voltage boundary violations are sufficiently penalised during the optimization step, the penalty coefficient has been determined as 300 through experimentation. The penalty coefficient was tested at 50 - 400 for all three test systems. As shown in the sensitivity results, changing the penalty value did not alter the optimisation outcome for CASE9 and CASE30; all coefficients produced identical L_{max} , power loss, and voltage deviation values. However, for CASE14, the penalty factor exceeded the voltage upper (1.08 pu.) limit in every case during the optimization behavior. Increasing the penalty factor by 100 times did not change the situation for case14; therefore, among the tested values, 300 provided lower power losses compared to the other factors and did not change the voltage violation level except for case14. Therefore, the 300 factor is presented as the appropriate value in terms of optimization speed.

3.3.3 Scenario-Based Performance Evaluation and Voltage Stability Analyses

The top 10 lines with the highest active power flow in the base case were identified, and these lines were sequentially de-energised in each scenario. For each fault event, the system's L_{max} value, power losses and voltage violations were calculated to assess the contribution of PV and ESS to system safety in quantitative terms. Two additional analyses were performed to investigate the system's resilience to voltage collapse in more depth:

- **Q-V Analysis:** The relationship between reactive power injection (Q) and bus voltage (V) at the

critical PV bus was investigated in the range from -150 to +250 MVar in 5 MVar steps.

- **P-V (CPF) Analysis:** System loads were gradually increased from 1.0 to 1.6 using the loading parameter λ , and the collapse limit λ_{max} was determined as the limit at which the power flow did not converge.

Parameter	Value	Description
α, β limits	[0.10–0.30], [0.05–0.18]	PV–ESS power ratios
w_1, w_2, w_3	0.60, 0.25, 0.15	Weighting factors
Population, Generations	40, 60	GA parameters
p_c, p_m	0.9, 0.02	Crossover and mutation
V_{min}, V_{max}	0.95–1.08 p.u.	Voltage limits
Penalty coefficient	300	Voltage violation penalty

Table 1: The values used in the study has been submitted in this form

4. RESULTS

The effect of the suggested approach on the system has been analysed comparatively under three main case studies:

1. **Base Case:** The existing (unmodified) reference condition of systems without any PV or ESS integration.
2. **+PV(opt):** The case where only an optimally located and sized PV system is added.
3. **+PV+ESS(opt):** The end state where an optimally located and sized integrated PV and ESS system, optimally positioned and sized using GA, is included, representing the full output of the proposed methodology.

TEST SYSTEM	OPTIMAL LOCATION (bus number)		OPTIMAL SIZE (MW)	
	PV	ESS	PV	ESS
CASE9				
Base case	-	-	-	-
Optimized	9	5	42.45	28.834
CASE14				
Base case	-	-	-	-
Optimized	9	14	77.7	42.475
CASE30				
Base case	-	-	-	-
Optimized	4	29	29.826	9.46
TEST SYSTEM	L_{max}	P_{loss} (MW)	Δ_{ava} (pu)	
CASE9				
Base case	0.15496	4.641	0.02298	
Optimized	0.067765	4.3151	0.023364	
CASE14				
Base case	0.076752	13.393	0.048473	
Optimized	0.019598	5.3777	0.059151	
CASE30				
Base case	0.055286	2.4438	0.018057	
Optimized	0.049905	2.0283	0.016011	

Table 2: Base case and optimisation results

Comparing the baseline case with the proposed integrated PV+ESS(opt) case, the proposed methodology improves the primary targets of voltage stability (L_{max}) and system efficiency (total active power loss- P_{loss}) significantly across all systems. Following the quantitative overview presented in Table 2, the effect of the proposed methodology on the voltage profile of systems under normal operation conditions is shown in Figure 1,2,3. This analysis demonstrates how GA optimization handles the mean voltage deviation (Δ_{ava}), one of the parameters in the aim function, and how it impacts the system's overall voltage quality.

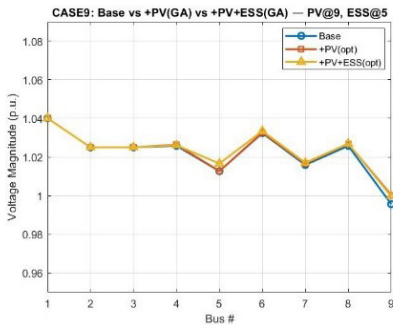


Table 2: Base case and optimisation results

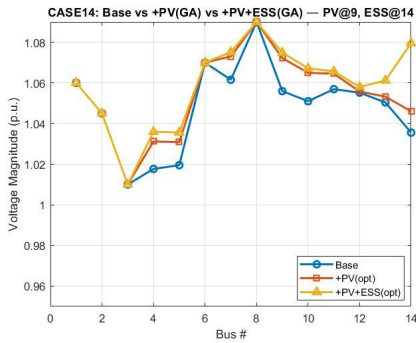


Figure 2: CASE14 voltage profile

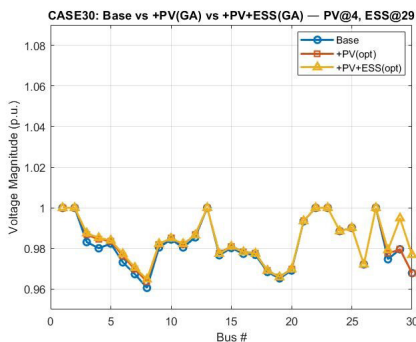


Figure 3: CASE30 voltage profile changes

Especially when considering CASE9 and CASE30, the voltage levels of weak bars (e.g. CASE9, Bus 9 and CASE30, Bus 8, 9, 30) that remain below 1.0 p.u. It is evident that the voltage ratings of weak bars (e.g. CASE9, Bar 9 and CASE30, Bars 8, 9, 30) that fall short of the nominal value are increased to or exceed the rated value through optimized PV and ESS

optimization.

Continuous Power Flow (CPF) analysis was performed to determine the system's resilience to voltage collapse and its limit of peak load ability. The resulting P-V curves indicate when the system reaches its voltage collapse point λ_{max} as the system load is increased gradually (λ loading parameter). Figure 4,5,6 shows a comparison of these PV results for the three test systems

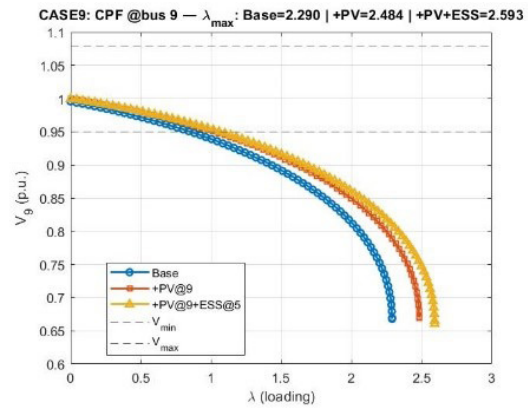


Figure 4: CASE9 changes in P-V curves

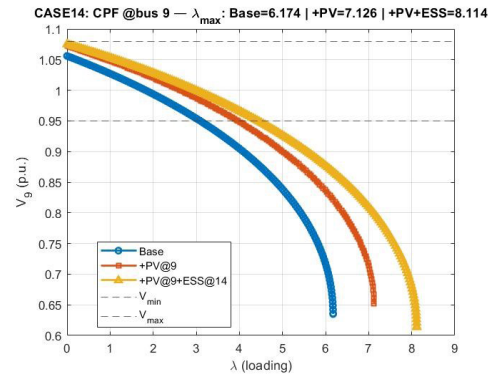


Figure 5: CASE14 changes in P-V curves

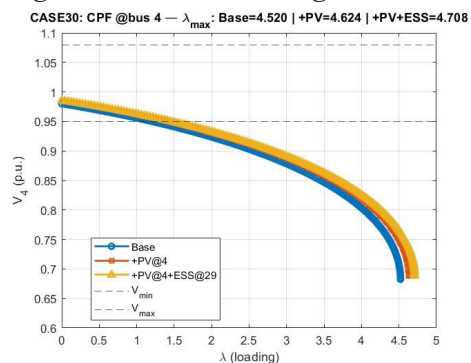


Figure 6: CASE30 changes in P-V curves

The CPF shows that PV and ESS integration improves stability margins by shifting the voltage collapse point to the correct side in all test systems. Careful examination of Figures 4, 5, and 6 shows that the PV+ESS integrated system is more stable than the base state. Figure 7,8,9 shows the maximum L_{max} values for each test system in the N-1 scenario. The algorithm was created by disabling the 10 lines with the highest power flow.

When the results of the N-1 emergency analyses are examined, it has been shown that the PV+ESS integrated system significantly increases reliability against serious faults.

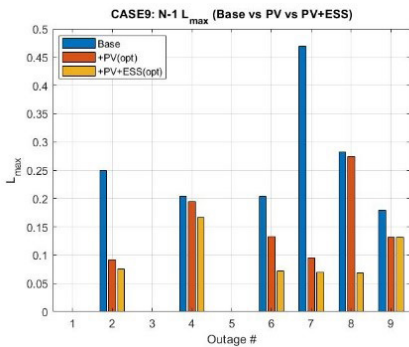


Figure 7: CASE9 N-1 emergency situation analysis

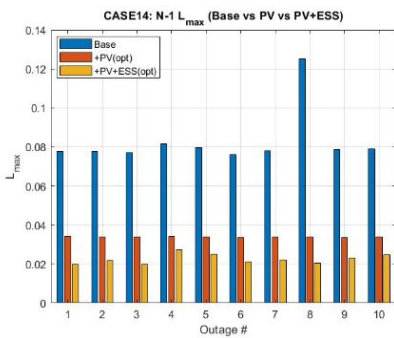


Figure 8: CASE14 N-1 emergency situation analysis

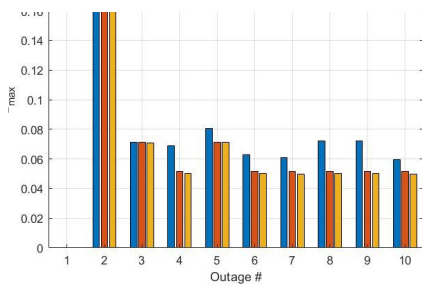


Figure 9: CASE30 N-1 emergency situation analysis

In conclusion, the proposed Genetic Algorithm-based PV+ESS optimization provides improvements in the stability, efficiency, and reliability of power systems. The results demonstrate that the methodology is effective not only in small systems but also in large-scale grids.

5. DISCUSSION AND SUGGESTIONS

This paper proposes a strategy that simultaneously addresses the voltage stability and resilience criteria for the integration of photovoltaic (PV) and energy storage systems (ESS) into power systems. The results demonstrate that the proposed Genetic Algorithm

(GA)-based method can significantly improve the system's performance results.

Analyses conducted on IEEE 9, 14, and 30-busbar systems demonstrate that the established model performs systematically. The results reveal that the L-index ratio increases by 57%, 74%, and 5% for 9, 14, and 30-busbar systems, respectively (Table 2).

The most notable performance was achieved in the IEEE 14-bus system, demonstrating the success of the methodologies. Thanks to optimal placement and sizing in this system, the maximum L-index (L_{max}) is reduced from 0.07675 to 0.01960, leading to a 74% improvement in stability. At the same time, the total active power loss (P_{loss}) was decreased from 13.393 MW to 5.3777 MW, thus achieving a 60% efficiency improvement in the system. The results of CASE 14 in this case also emphasize the efficiency of the multi-objective Genetic Algorithm (GA). GA achieved this improvement in the L_{max} and (P_{loss}) metrics, the GA made a considered trade-off decision to increase the average voltage deviation (Δ_{avg}) from 0.048 to 0.059. This shows that GA allows for a slight voltage deviation from 1.08 while reducing losses. The algorithm allows for a slight voltage deviation from the reference value while achieving the highest L_{max} gain and the lowest P_{loss} objective. Similarly, in CASE 9, L_{max} increased by 57% while P_{loss} decreased by 8%, and in CASE 30, L_{max} increased by 5% while P_{loss} decreased by 11%, showing significant improvements.

The CPF shows that improvement is most dramatic in CASE14. The maximum load limit of the system, which was $\lambda_{max} = 6.174$ in the basic case, has been improved to $\lambda_{max} = 8.114$ thanks to the optimized PV and ESS integration. This result shows that the amount of load that the system can carry increases by 31.4%. Similarly, the stability margin increased by 13.2% in CASE 9. It increased by 4.15% in CASE 30. These findings indicate that strategically positioned and sized PV and ESS integrated cases directly increase resilience to voltage drops. In CASE 9, in the scenario of line 7 breaking, the base case reaches a hazardous level of 0.47, which brings the system closer to the voltage collapse boundary. In contrast, the PV+ESS(opt) case almost completely absorbs the impact of this critical failure by reducing it to 0.07, thus keeping the system in a secure operating state. Likewise, significant drops in the index are obtained for the 2nd, 6th, and 8th line breaks. A similar success was achieved in CASE 14. Line 8 is the most risky line. While $L_{max} \approx 0.125$ in the base case, the PV+ESS algorithm decreased it to $L_{max} \approx 0.02$. CASE 30, IEEE 30-bus system already has high stability. The proposed PV+ESS optimization has increased the stability of this system.

Overall, these results show that coordinated placement and sizing of PV and ESS significantly improve both stability and resilience. The proposed method adapts successfully to different system structures and stress

conditions.

Moreover, the proper positioning and sizing of PV and ESS significantly improves the system's stability and voltage quality. Nevertheless, if integration increases irregularly, the system's dynamic stability and reactive power balance can be adversely affected. Since the proposed approach is based on static power flow and steady-state voltage stability indicators, it does not capture the system's dynamic behaviours such as frequency response, transient voltage recovery, or inverter control interactions. This constitutes a natural limitation of the present methodology. For this reason, future studies should also investigate in detail the effects of increasing renewable penetration on the system's dynamic parameters.

6. REFERENCES

- Ülger, A. B., & Dağ, O. (2024). Mikro şebekelerde arıza durumunda kararlılık analizi. *Disiplinlerarası Yenilik Araştırmaları Dergisi*, 4(2), 128-145.
- Kundur, P. (1994). *Power system stability and control*. New York: McGraw-Hill.
- Tachibana, M., Palmer, M. D., Senjyu, T., & Funabashi, T. (2014). Voltage stability analysis and (P,Q)-V characteristics of multi-bus system. *CIGRE AORC Technical Meeting*, 1–6.
- Wu, Y.-K. (2007). A novel algorithm for ATC calculations and applications in deregulated electricity markets. *International Journal of Electrical Power & Energy Systems*, 29(10), 810–821.
- Ajjarapu, V., & Lee, B. (1998). Bibliography on voltage stability. *IEEE Transactions on Power Systems*, 13(1), 115–125.
- Stanković, A. M., Tomšović, K. L., De Caro, F., Braun, M., Chow, J. H., Čukalevski, N., ... Zhao, S. (2022). Methods for analysis and quantification of power system resilience. *IEEE Transactions on Power Systems*, 38(5), 4774–4787.
- Abdolahi, A., Samadi Gharehveran, S., & Shirini, K. (2025). Optimizing energy storage solutions for grid resilience: A comprehensive overview. In A. Y. Abdelaziz, M. A. Mossa, & M. Bajaj (Eds.), *Energy Storage Devices—A Comprehensive Overview*. Rijeka, Croatia: IntechOpen.
- Zhao, Y., Zhang, T., Sun, L., Zhao, X., Tong, L., Wang, L., ... Ding, Y. (2022). Energy storage for black start services: A review. *International Journal of Minerals, Metallurgy and Materials*, 29(4), 691–704.
- Aslam, M. U., Miah, M. S., Amin, B. R., Shah, R., & Amjady, N. (2025). Application of energy storage systems to enhance power system resilience: A critical review. *Energies*, 18(14), 3883.
- Gao, B., Morison, G. K., & Kundur, P. (1993). Voltage stability analysis using static and dynamic approaches. *IEEE Transactions on Power Systems*, 8(3), 222–231.
- Ekinci, S. (2015). Simulink kullanarak güç sistem geçici hâl kararlılık analizi. *Sakarya Üniversitesi Fen Bilimleri Dergisi*, 19(3), 118–127.
- Hsiao, Y.-T., Chiang, H.-D., Liu, C.-C., & Chen, Y.-L. (1994). A computer package for optimal multiobjective VAR planning in large-scale power systems. *IEEE Transactions on Power Systems*, 9(2), 668–676.
- Chen, Y.-L., & Liu, C.-C. (1994). Multiobjective VAR planning using the goal-attainment method. *IEEE Proceedings – Generation, Transmission and Distribution*, 141(3), 227–232.
- Xiong, H., Cheng, H., & Li, H. (2008). Optimal reactive power flow incorporating static voltage stability based on multi-objective adaptive immune algorithm. *Energy Conversion and Management*, 49(5), 1175–1181.
- Ramasamy, A. K., Verayiah, R., Abidin, I. Z., Gunalan, P., & Perumal, S. (2016). Study on P–V curve and V–Q curve of an unbalanced three-phase system with different static loads. *Przełąd Elektrotechniczny Conference Proceedings*, 1–6.
- Al Jabri, Y., Hosseinzadeh, N., Al Abri, R., & Al Hina, A. (2015). Voltage stability assessment of a microgrid. *Proceedings of the 8th IEEE GCC Conference and Exhibition*, 1–6.
- Zare, A., & Kazem, A. (2007). Use of PQV surface as a tool for comparing the effects of FACTS devices on static voltage stability. *International Journal of Energy*, 4(1), 223–228.
- Overbye, T., & Dobson, I. (1994). Q–V curve interpretations of energy measures for voltage security. *IEEE Transactions on Power Systems*, 9(1), 128–132.
- Chen, G., Liu, L., Song, P., & Du, Y. (2014). Chaotic improved PSO-based multi-objective optimization for minimization of power losses and L-index in power systems. *Energy Conversion and Management*, 86, 548–560.
- Taylor, C. W. (1994). *Power system voltage stability*. New York: McGraw-Hill.
- Leonardi, B., & Ajjarapu, V. (2013). An approach for real-time voltage stability margin control via reactive power reserve sensitivities. *IEEE Transactions on Power Systems*, 28(2), 615–625.
- Cho, K. H., Kim, J., Byeon, G., & Son, W. (2024). Optimal sizing strategy and economic analysis of PV–ESS for demand side management. *Journal of Electrical Engineering & Technology*, 19(5), 2859–2874.
- Liu, Y., Zhong, Y., & Tang, C. (2023). Sizing optimization of a photovoltaic hybrid energy storage system based on long time-series simulation considering battery life. *Applied Sciences*, 13(15), 8693.
- Qi, H., Yan, X., Kang, Y., Yang, Z., Ma, S., & Mi, Y. (2024). Multi-objective optimization strategy for the distribution network with distributed photovoltaic and energy storage. *Frontiers in Energy Research*, 12, 1418893.
- Wang, Z., Luo, Y., Wu, W., Cao, L., & Li, Z. (2025). Multi-objective optimization models for power load balancing in distributed energy systems. *Energy Informatics*, 8(1), 104.